Longitudinal Tomographic Reconstruction of LHC-type Bunches in the SPS

T. Bohl, H. Damerau, S. Hancock

Summary

Longitudinal tomographic reconstruction on the basis of measured profiles is an important technique to measure the particle density distribution of a bunch in longitudinal phase space. This measurement technique, well established in all circular machines of the PS complex, has been applied to the SPS for the first time. Due to recent improvements of the data acquisition of the signals from the longitudinal pick-ups in the SPS and a new LHC type wall current monitor, the quality of the bunch profiles is now more appropriate for tomography. Longitudinal beam signals from the wall current pick-ups APWL-10 and WC-2 are used as input for the reconstruction algorithm. It is shown that, due to short bunches and long cables in the SPS, the correction of the signal with the transfer function of the transmission system is indispensable. The analysis of the longitudinal distribution of a batch of 48 bunches of an LHC type beam at injection into the SPS, averaged over more than ten cycles, showed that any systematic variation of the bunch parameters along the batch is shadowed by statistical errors due to the quality of the measured bunch profiles. Avoiding the long coaxial cables from the SPS tunnel to the surface is a crucial issue for improving the quality of the bunch profiles suitable for tomographic reconstruction.

1   Introduction

Longitudinal tomographic reconstruction on the basis of measured profiles is an important technique to reconstruct the particle density distribution of an arbitrary bunch in longitudinal phase space. In addition to visualizing a bunch in the longitudinal plane, the knowledge of the particle distribution permits the calculation of several parameters, e.g., longitudinal emittance and momentum spread, with a much better precision than is possible from the observation of a bunch profile. Longitudinal tomography at CERN was originally developed to investigate the complex RF manipulations in the PS [1, 2], but it is now a well-established operational tool in all machines of the PS Complex: AD, LEIR, PSB and PS [3].

The reconstruction method relies on the rotation of a particle distribution in longitudinal phase space due to synchrotron motion. Each of the measured bunch profiles provides a projection of the distribution at a certain phase of the synchrotron oscillation. The combination of a sufficiently large number of projections at different phases of the rotation permits a good approximation to be found to the longitudinal distribution generating those profiles. The result after sufficient iterations is a 2D distribution that is consistent with all the measured profiles and the laws of synchrotron motion and, hence, yields the bunch parameters more precisely than a single profile.

Due to significant capture losses in the SPS, the longitudinal distribution of the LHC beam at transfer from PS to SPS is of special interest. However, the Tomoscope in the PS cannot be used in this case because the data acquired during the bunch rotation, which takes place during one quarter of a synchrotron

period prior to extraction, is not sufficient for tomography. The extraction from the PS can be delayed to prolong the rotation and to record more profile data, but in doing so the longitudinal beam quality is badly compromised and unusable for further acceleration in the SPS. More favorable conditions to record profiles for tomography exist in the SPS during the first turns after injection.

Shortly after its invention, the reconstruction technique was tried in other machines than the PS. However, in the SPS, the first attempts performed in 1997 were not very encouraging, mainly due to the distortion of the signals due to the combination of short bunches and long cables. As the bunch signal acquisition in the SPS has been significantly improved since these first tests, new data suitable for tomographic reconstruction have been taken during MDs in September 2006. The analysis of these measurements and their results are described in this Note. It is shown that relevant information on the emittance and tilt angle of LHC bunches at injection into the SPS can be retrieved by means of tomography. Limitations are discussed as well as possible improvements.

2   Transfer function correction

There are two main differences between the accelerators in the PS complex and the SPS. Firstly, bunches in the SPS are accelerated with an RF system at 200 MHz and the natural bunch length is much shorter than in the PS where acceleration and RF manipulations take place with RF systems in the frequency range of $3 - 40$ MHz. Secondly, the longitudinal beam signal from a wall current monitor is digitized close to the ring (approximately 35 m of 7/8" coaxial cable) in the PS, whereas the signals from the wall current monitors in the SPS are transferred from the ring tunnel to the surface where they are finally digitized. This results in a considerable length of the coaxial cables of about 200 m. While the signal distortion introduced by the transmission system in the PS is at the limit of what can be detected, the signal distortion in the SPS is so large that a correction of signals for the transfer function of the transmission system is indispensable.

As tomography assumes that particle distributions in the longitudinal phase space vary with time according to the laws of synchrotron motion, it can be disturbed by base line drifts of the signal or ripple on the bunch profiles. Such perturbations do not develop according to these laws, since they are not due to a physical density distribution. However, the tomographic algorithm tries to find a physical distribution representing the ripple and the baseline drift, which fails inevitably.

Therefore, the inverse transfer function of the measurement system, from the wall current pick-up (APWL-10 and WC-2) to the digital oscilloscope has been applied to the measured profiles to correct for the distortion. Especially dispersion and attenuation of the cables contribute significantly to the difference between real beam signal and the signal that is digitized on the surface. Though this ripple and ringing behind the sharp peak of a short bunch is not of major relevance for bunch length measurements, as the error introduced by cable dispersion is nearly constant for a certain range of bunch lengths, it turns out to be unacceptable for input data for a tomographic reconstruction.

The transfer function of the transmission system is compensated in the frequency domain. The measured bunch signal from a longitudinal pick-up consisting of a list of n measured points (t_i, a_i), where t is time and a is amplitude, is firstly converted to the frequency domain by a Fourier transform. This transformation results in a list of Fourier components $(c_0, c_1, \ldots, c_n)$. Since the measured signal is real, the second half of the Fourier components contains redundant information as

$$
\begin{aligned}
(c_0, c_1, \ldots, c_n) &= (c_0, c_1, \ldots, c_{n/2}, c_{n/2+1} = c_{n/2}^*, \ldots, c_n = c_1^*) \quad \text{for even } n \text{ or} \\
(c_0, c_1, \ldots, c_n) &= (c_0, c_1, \ldots, c_{(n+1)/2-1}, c_{(n+1)/2}, \\
&\quad\quad c_{(n+1)/2+1} = c_{(n+1)/2-1}^*, \ldots, c_n = c_1^*) \quad\quad \text{for odd } n \, .
\end{aligned}
\tag{1}
$$

An odd (n even) number of points has been implemented into the transfer function correction only. For even (n odd) length of the time domain input data, the final point is removed from the data. The loss of

a single data point can be accepted as a data trace typically contains several thousand points.

The Fourier components c_0 to $c_{n/2}$ are then multiplied with the inverse transfer function of the longitudinal pick-up and the transmission system including all cables and hybrids. The measured transfer function of the new longitudinal wall current monitor (APWL-10) is almost completely flat in the relevant frequency range and its correction has no significant effect on the bunch signal. Therefore, only the distortion due to cable transfer function has been corrected for that pick-up. The explicit transfer functions for wall current monitor pick-up APWL-10 and WC-2, as well as the transfer functions of the transmission systems are given in the appendices.

The transmission system, due to its long cables from the ring tunnel to the surface, has a large attenuation at high frequencies and the high frequency Fourier components are strongly amplified by the cable correction. This leads to significant high frequency noise on the corrected bunch signal. Therefore, the spectrum is cut around 2 GHz. Smooth attenuation of higher frequencies similar to a low-pass filter have also been tried, but the results are not superior compared to replacing all Fourier components above the frequency by zero.

After reconstruction of the Fourier components $c_{n/2+1}$ to c_n according to Eq. (1), the component list is inversely Fourier transformed to get the corrected signal in time domain. By definition the resulting signal is real. The effect of the transfer function correction on one bunch is illustrated in Fig. 1. One
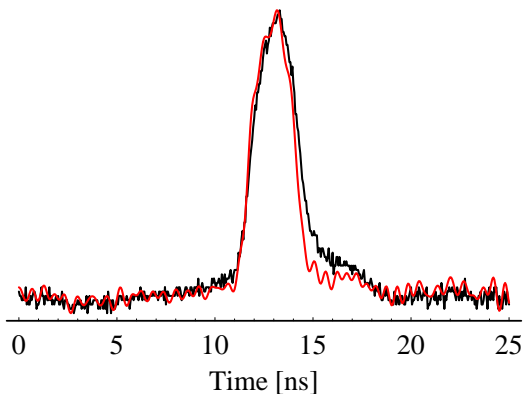

Fig. 1: Bunch signal recorded with the wall current pick-up WC-2 before (black) and after correction (red) with the transfer function of pick-up and cable. The data are normalized to allow for the direct comparison.

can clearly see that the tail behind the bunch is suppressed by the correction as it comes mainly from cable dispersion. As the relevant information for tomography is within the duration of one bucket, which corresponds to 5 ns in the SPS, the transfer function correction is indispensable.

3 Data preparation for tomography

Longitudinal phase space tomography is implemented as an online application, the so-called Tomoscope [3], throughout the PS Complex. The longitudinal phase space distribution is calculated and displayed together with a list of bunch parameters on a single-button basis. The original offline program for tomographic reconstruction takes the same input data as the online application and remains available in addition. The online application acquires the mountain range data and all the relevant machine parameters, like bending field and RF voltages, entirely automatically. All the data may be saved to file from the application for archive purposes. Since such files can also be read back into the application, they may be used to feed mountain range data from the SPS into the Tomoscope application of the PS for processing. A *Mathematica* notebook has been developed to perform this file conversion automatically. An example of the bunch data recorded with a Tektronix TDS7254 digital oscilloscope is shown in Fig. 2.

Firstly, the transfer function correction as described above is performed. Thereafter, the long traces are cut into data belonging to single bunches. A large fraction of the recorded data is eliminated at this stage. For the LHC type beam the bunch spacing of 25 ns is well above the length of the bunches
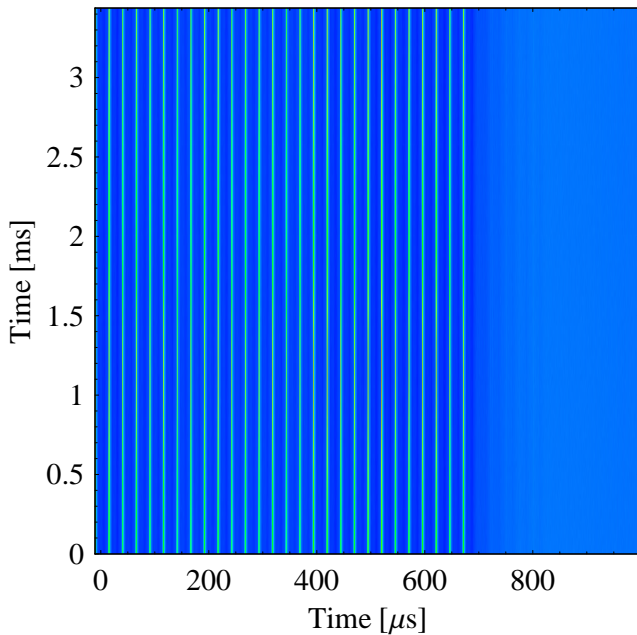
Fig. 2: Mountain range density plot of the bunches 22 to 48 during the first 150 turns of an LHC type batch with 48 bunches in the SPS. The sampling rate of the bunch signal is 20 GS/s and a frame of data is taken every turn. The total intensity was about $3 \cdot 10^{12}$ ppp ($6.3 \cdot 10^{10}$ ppb).

and a time window of 10 ns is imposed, of which only from 5 to 7 ns are taken for the phase space reconstruction.

Of major importance for the correct tomographic reconstruction is the position of the synchronous phase (stable fixed point) with respect to the bunch data [3]. In the online version of the Tomoscope, the fixed point can either be estimated from the bunch profile using a foot tangent algorithm or entered manually. For the data taken in the SPS the synchronous point was calculated from the average over the center positions of a Gaussian fit to each individual bunch.

After that, the *Mathematica* notebook generates a directory structure containing files which are directly suitable for importation into the online Tomoscope application or for processing with the offline tomographic reconstruction code. Fig. 3 shows a typical screen shot of a mountain range of an SPS bunch imported into the PS Tomoscope. All relevant parameters for the reconstruction are calculated automatically within the *Mathematica* conversion notebook.
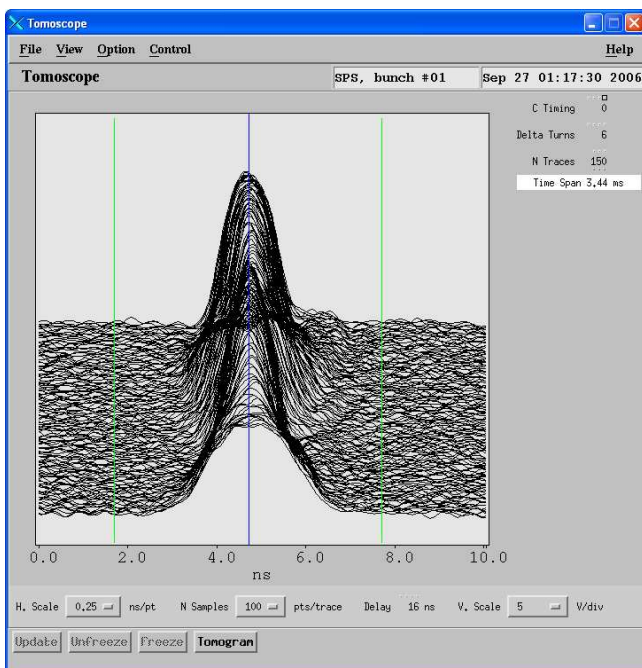

Fig. 3: Single bunch of an LHC type beam measured in the SPS and imported into the online Tomoscope application of the PS. The blue line indicates the stable fixed point position calculated with the algorithm described in this section. The green lines show the limits of the data taken into account for the tomographic reconstruction. Their positions are defined from the bucket length.

4

However, it is worth mentioning that the use of the calculated synchronous point from Gaussian fits might not always be the optimum. This is illustrated by the two phase space reconstructions shown in Figs. 4 and 5 based on the data from Fig. 3. Note that the absolute beam intensity is not calibrated
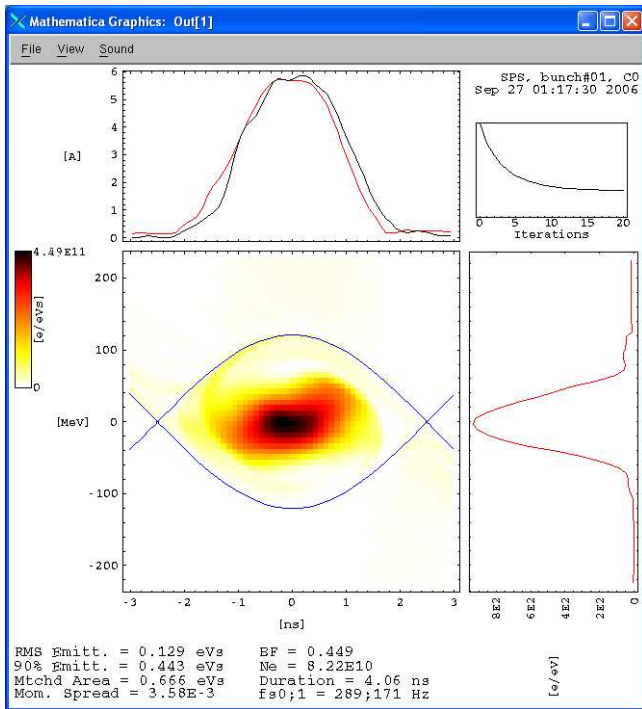

Fig. 4: Tomographic reconstruction of longitudinal phase space based on the bunch profiles illustrated in Fig. 3 using the automatically calculated stable fixed point position.
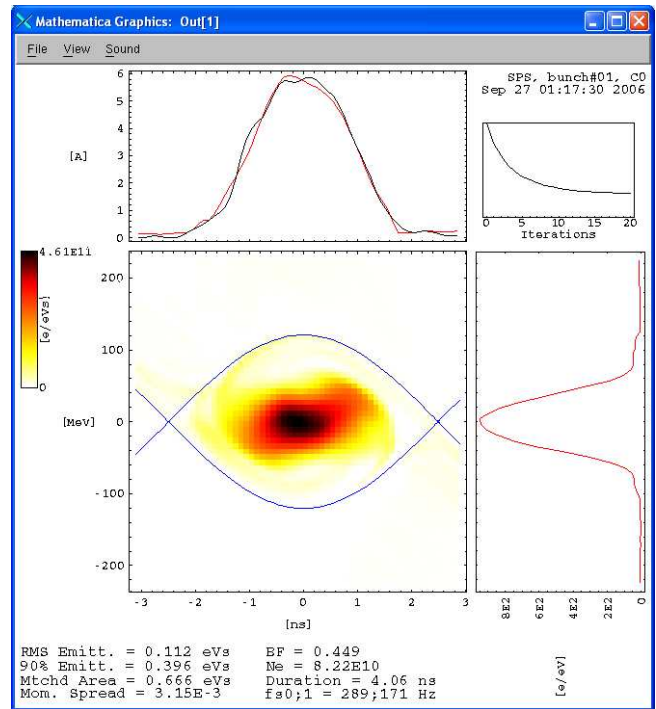
Fig. 5: Tomographic reconstruction of the same profile data as in Fig. 4. The stable fixed point is shifted to the right by about $100\,\mathrm{ps}$ which improves the convergence of the image.

and that the scaling of the projected plots is consequently erroneous. Clearly, the bunch profile from the reconstructed distribution (red trace of the graphs on top of the phase space) is displaced with respect to the measured bunch profile (black trace) in Fig. 4. Adjusting this manually results in the longitudinal phase space distribution shown in Fig. 5. The shift between reconstructed and measured bunch profiles has been removed. Moreover, the convergence (upper right plot), which is an independent parameter to quantify the quality of the reconstruction, is slightly better for the second plot. Both convergence plots in Figs. 4 and 5 have the same vertical scaling.

4 Development of the bunch parameters along the batch

Applying tomography to each of the individual bunches of a single shot results in the longitudinal phase space distribution along the batch. The bunch parameters, especially the longitudinal emittances can be computed with a better precision than directly from the measured profiles. However, the influence of the tails of the reconstructed distributions may decrease the precision of the emittance measurement. An example for the reconstructed phase space for all 48 bunches at injection into the SPS is shown in Figs. 6 and 7. The beam intensity was about $3 \cdot 10^{12}\,\mathrm{ppp}$ and the RF voltage at capture has been set to $2.3\,\mathrm{MV}$. The data for the reconstructions of the first 24 bunches have been recorded during a single shot. The data for the second half of the batch have also been recorded during one cycle, but about 30 minutes later, without changing the beam conditions. The parameters of the tomographic reconstructions may not be perfectly optimized for each bunch, but as some 450 bunches were processed, automatic procedures were favored in comparison with manual parameter optimization.
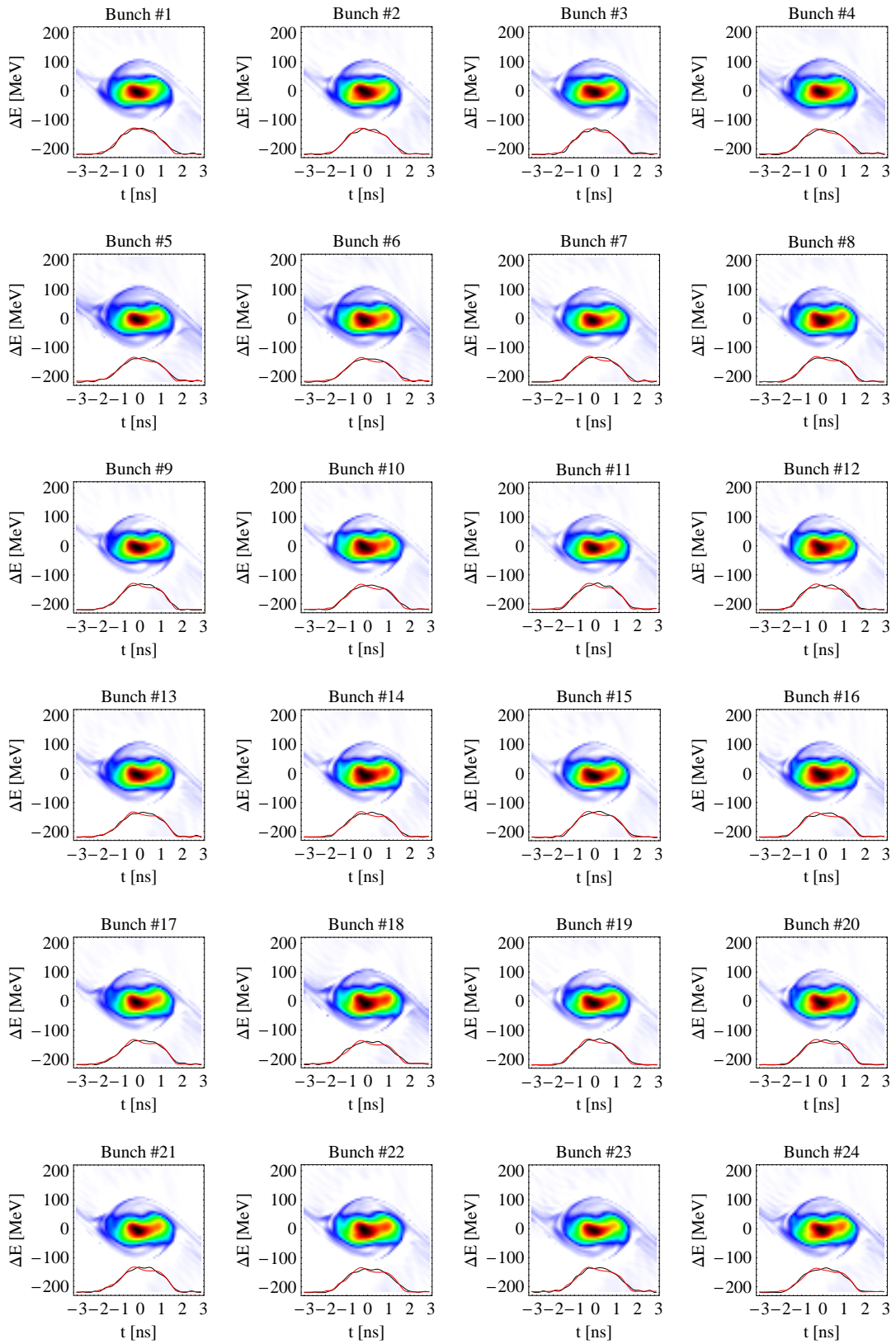
Fig. 6: Tomographic reconstruction of the first 24 LHC type bunches of a batch of 48 bunches in total. The profile data have been recorded during the first 150 turns after injection with wall current pick-up WC-2.

Fig. 7: Tomographic reconstruction of the last 24 LHC type bunches of a batch of 48 bunches in total. The profile data have been recorded during the first 150 turns after injection with wall current pick-up WC-2.
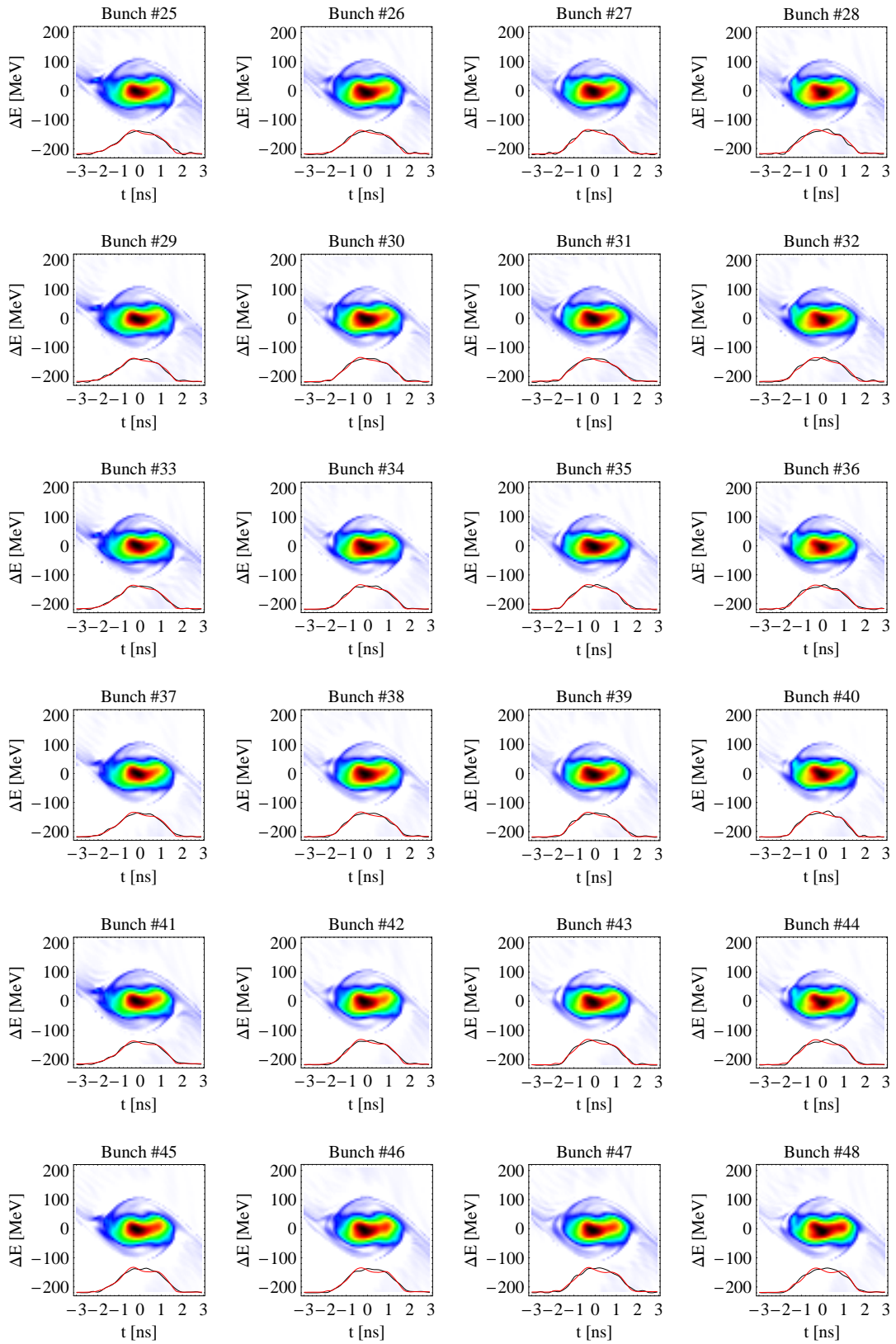
To produce short bunches for the LHC with $4\sigma \simeq 4$ ns in the PS, the bunches are rotated during a quarter of a synchrotron period. At extraction, when the bunches are shortest, they should be upright. The window for a good extraction is only a few turns long. However, as the synchrotron frequency depends on the voltage during bunch rotation, the amount of rotation applied to the individual bunches along the train is not necessarily the same. Measurements of the gap voltage of the cavities used for the bunch rotation in the PS showed that its variation is small, but there are currently no means to measure the amount of rotation along the batch in the PS.

From the tilt angle of the bunches in Figs. 6 and 7 it can be clearly seen that all bunches are rotated comparably in the PS. All bunches are observed to be in the horizontal position in the SPS and no tilt angle from bunch-to-bunch can be identified. As is shown in the subsequent paragraph, the absolute tilt angle of a mismatched bunch cannot be deduced from a reconstructed distribution with high precision, but only the bunch-to-bunch variations.

The knowledge of the distribution of the bunches in the longitudinal phase space enables the derivation of the longitudinal emittance in any definition. This results in emittance figures which are independent of, for example, quadrupole oscillations which would degrade the precision of emittance values deduced from the bunch length. Although the RMS emittance does not intuitively represent the area in longitudinal phase space occupied by the bunch, it can be directly calculated for any kind of distribution. It therefore allows bunch-to-bunch emittance variations along a batch to be assessed. To determine whether these variations can be attributed to the real bunch parameters along the batch or if they are due to statistical errors of the measurement, it has been tried to correlate the emittance from the tomographic reconstruction along the batch with bunch length and bunch intensity (Fig. 8). The upper left plot shows the 4σ bunch length from a Gaussian fit to the profile of the time instant of the reconstruction. The longitudinal RMS emittance along the batch is plotted in the lower left diagram. To reveal possible correlations between bunch length and RMS emittance, both curves have been normalized and plotted together in the upper diagram in the center of Fig. 8. Longitudinal emittance versus bunch length is shown in the upper plot on the right. Finally, longitudinal RMS emittance is also plotted versus integrated bunch intensity and the maximum bunch amplitude from the Gaussian fit on the lower diagrams in the center and on the right. None of the plots discloses a significant correlation between longitudinal RMS emittance, bunch length or bunch intensity. Moreover, the bunch-to-bunch variation of the measured RMS emittance does not correspond to any typical pattern that could be generated in the PS due to asymmetries of the bunch splittings. The quality of the measured beam profiles was thus not sufficient to measure the real variation of the longitudinal emittance along the batch, as the real deviations are assumed to be covered by the statistical error. Neglecting the tails of the distribution and calculating the area in longitudinal phase space containing 90% of the particles reveals a slight correlation of the emittance and the bunch length along the batch. Cutting the tails of the bunch distribution is arbitrary, though.

The longitudinal RMS emittance along the batch, calculated from the reconstructed bunch distributions and averaged over several machine cycles is presented in Fig. 9. The black points show results from individual measurements and the red points are the averages over several injections. The upper plot gives the results of the measurements taken on 27/09/2006 with the WC-2 pick-up and the center plot those recorded with APWL-10 about an hour later. Only data of the first and the last six bunches have been recorded on 27/09/2006 with the latter pick-up. The lower plot presents the measurement of the full batch of 48 bunches measured on 29/09/2006 with the APWL-10 pick-up. The longitudinal RMS emittances suggested by the measurements taken with APWL-10 are consistent with those calculated from measurements recorded with WC-2.

The spread of the tomographic emittance measurements under the conditions in the SPS is about $\pm 15\%$. Due to the quality of the large bandwidth beam signal and its transfer function correction, the typial emittance error is larger than the few percent uncertainity [3] in the emittance calculation for the Tomoscope used in the PS Complex. Bunch-to-bunch variations are shadowed by the statistical error of the measurements.
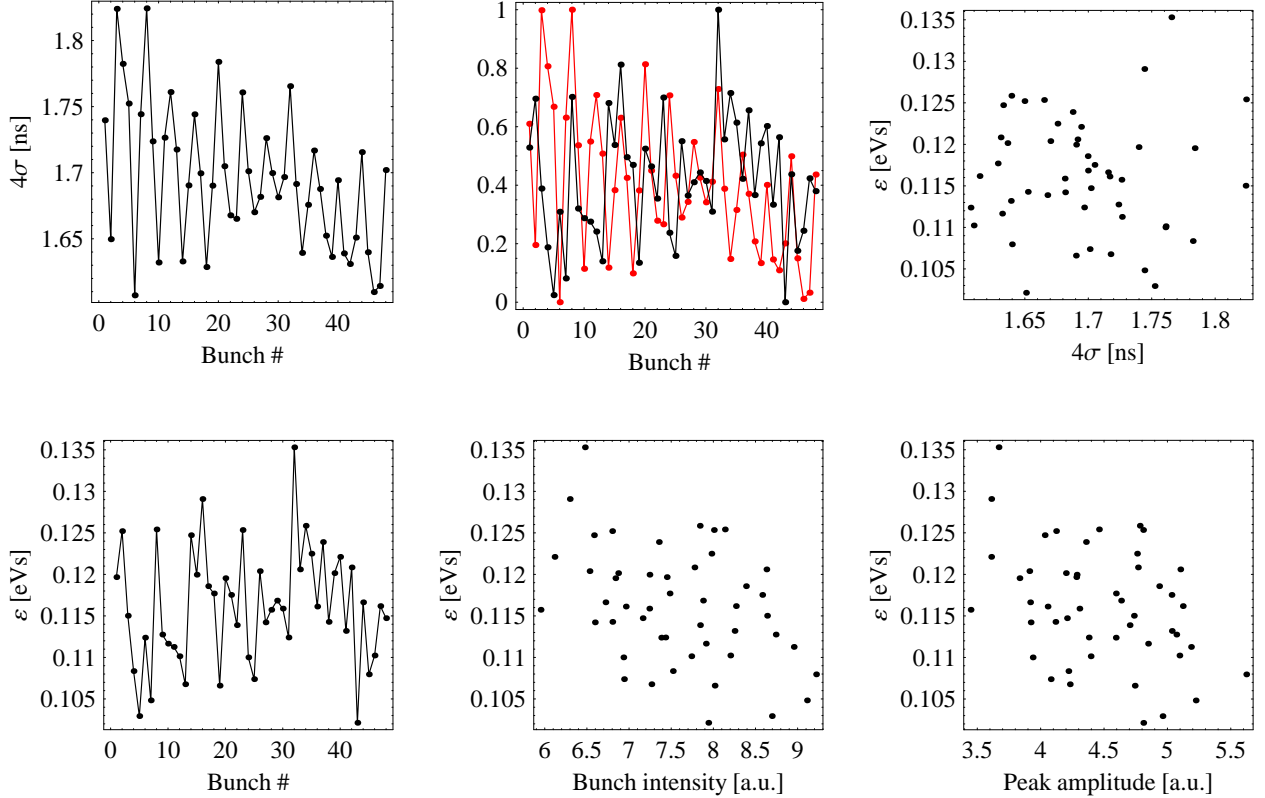
Fig. 8: Bunch length (upper left) and RMS emittance (lower left) along the batch of 48 bunches of a single measurement. Both graphs (red: longitudinal emittance, black: bunch length) are normalized and plotted together (upper center), but no significant correlation is observed. The RMS emittance is additionally plotted against bunch length (upper right), bunch intensity (lower center) and peak amplitudes of the bunches from the Gaussian fit (lower left). The bunch distributions have been topographically reconstructed at a quarter period of the synchrotron oscillation after injection which explains the short bunch lengths.

5 Sensitivity of the tomographic reconstruction

The tomographic reconstruction relies on measured bunch profiles and is based on the laws of synchrotron motion. A large number of particles is tracked in the longitudinal phase space to calculate maps describing the redistribution of longitudinal phase space during the measurement time. This should be at least half a synchrotron period. Consequently, several machine parameters, magnetic bending field and RF voltage amongst them, have to be fed into the Tomoscope. While most of these parameters are well-known or can be measured with a very high precision, the RF voltage in the SPS can be measured with a precision of only about $10\,\%$. Moreover, beam loading causes a bunch-to-bunch modulation of the RF voltage of the same order of magnitude. A wrong assumption for the RF voltage, V_{RF}, has two main effects on the resulting tomographic reconstruction.

Firstly, the bucket area of a stationary bucket scales like $\sqrt{V_{\mathrm{RF}}}$. The resulting longitudinal emittance, ε from the reconstruction will thus be wrong by a factor of $\varepsilon/\varepsilon_0 = \sqrt{V_{\mathrm{RF}}/V_0}$, where ε_0 is the correct longitudinal emittance for the correct RF voltage, V_{RF}. An error of $10\,\%$ in the assumption of the RF voltage leads to an emittance error of approximately $5\,\%$. Secondly, as the synchrotron frequency also scale with $\sqrt{V_{\mathrm{RF}}}$, the tomographic reconstruction may reflect the longitudinal phase space distribution at a wrong instant in time. This becomes relevant when mismatched bunches rotating in longitudinal phase space are analyzed, like at injection into the SPS. An error in the RF voltage introduces an erroneous tilt of the reconstructed bunch.
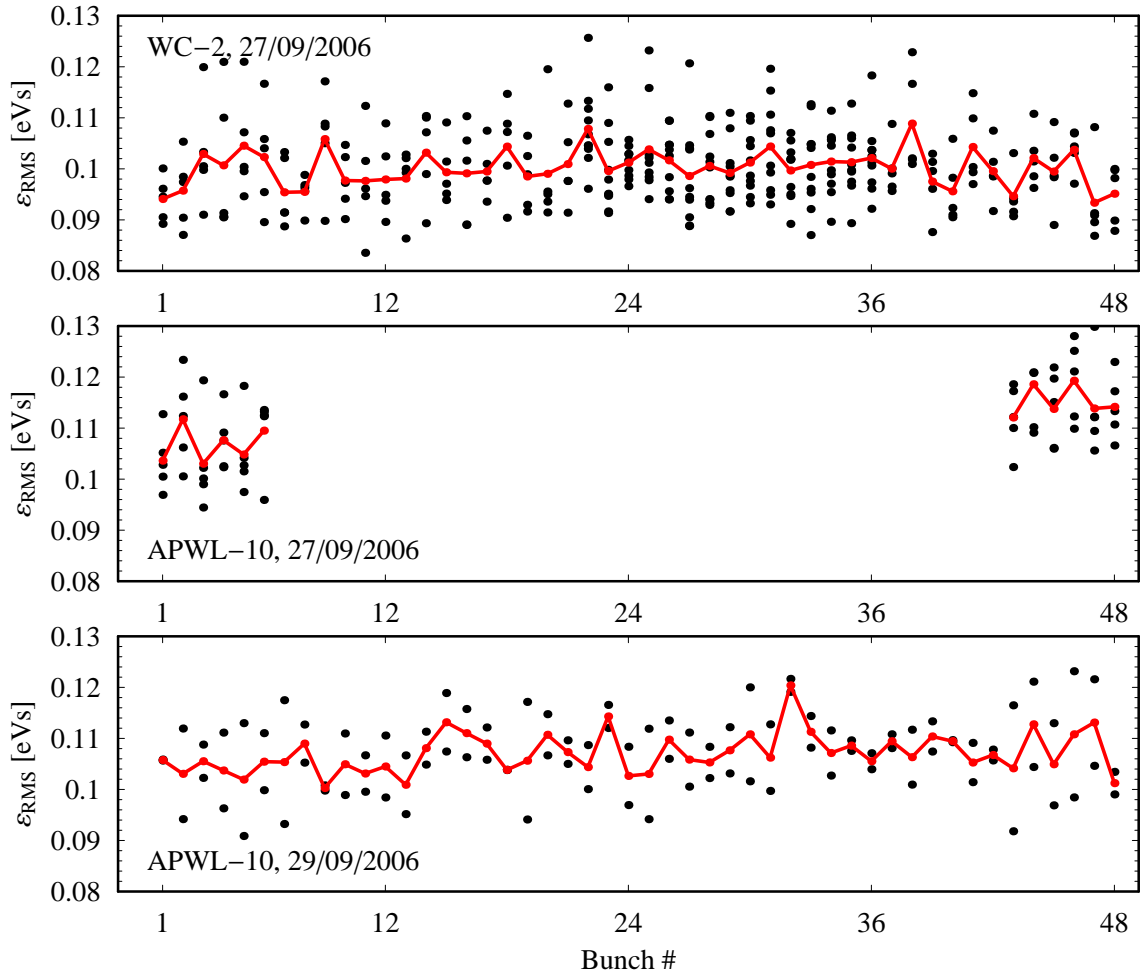
Fig. 9: RMS emittance along a batch of 48 bunches at injection in the SPS.

Both effects are illustrated in Fig. 10, assuming a voltage error far above the expected 10 %. The tilt angle of the bunch changes with the RF voltage as well as the scaling of the reconstructed longitudinal phase space. The plot range of the energy axis varies according to the voltage used in each reconstruction.

Though the RF voltage may not be known with the required precision for a precise tomographic phase space reconstruction, it is directly visible in e.g. the left upper plot of Fig. 10 that the phase space distribution is not realistic. Since the Tomoscope program calculates a discrepancy parameter indicating the quality of the reconstruction by comparing the measured bunch profiles with the profiles from the result of the reconstruction, certain input parameters can be optimized by monitoring their influence on convergence. As an example, discrepancy is plotted in Fig. 11 against the RF voltage used for the reconstructions of Fig. 10. This confirms that the bunches from the PS are upright at extraction from the PS and that the timing of the bunch rotation was thus correct when the data were recorded. (Due to the different aspect ratio of longitudinal phase space at injection in the SPS, the same bunches are horizontally aligned rather than vertically upright.) However, improving convergence by minimizing discrepancy is tedious; for each point of the discrepancy parameter plot in Fig. 11 one tomographic reconstruction must be processed.
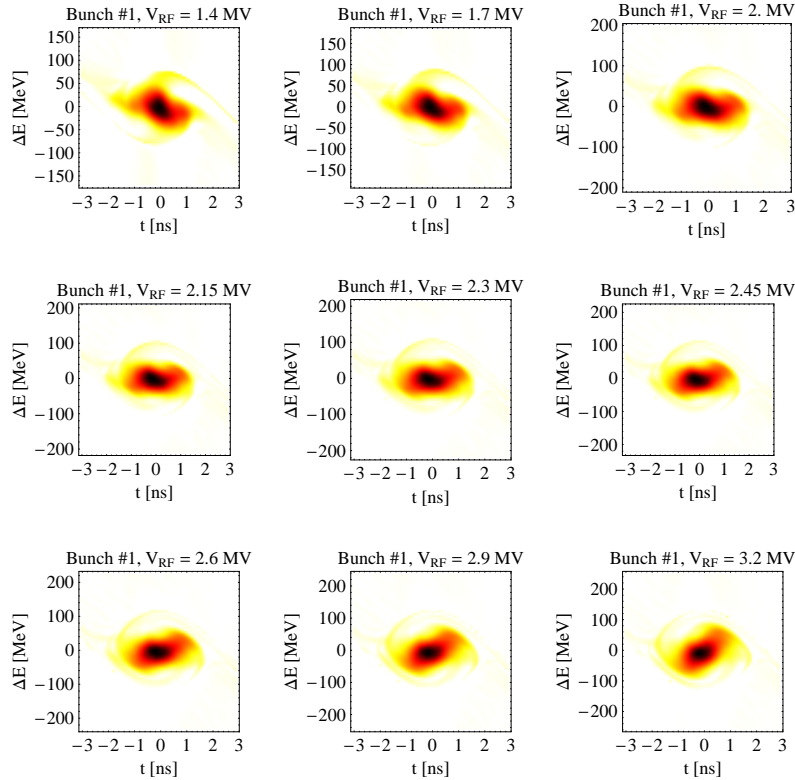
Fig. 10: Longitudinal reconstruction of the first bunch of an 48 bunch train at injection into the SPS, assuming various RF voltages from 1.4 to 3.2 MV. The measured value of the RF voltage is 2.3 MV.
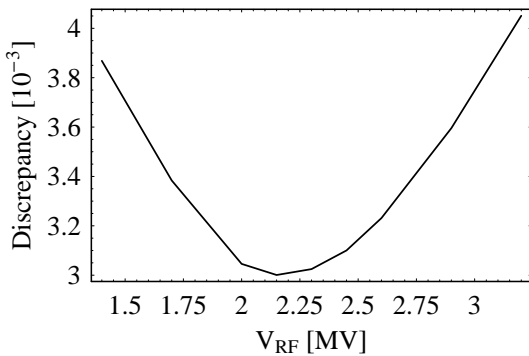

Fig. 11: Discrepancy parameter versus RF voltage assumed for the tomographic reconstructions in Fig. 10. As indicated by the phase space distributions, the real bunches are best represented for $V_{\mathrm{RF}} = 2.2$ MV, close to the measured value.

6 Conclusions

Mountain range bunch signals of the first 150 turns of a batch of 48 LHC bunches have been acquired during two MDs in September 2006. The longitudinal bunch distributions were reconstructed applying the longitudinal tomography code used in the PS Complex. The transfer function correction for the measurement system, especially those for the coaxial cables from the wall current monitors (APWL-10 and WC-2) in the tunnel to the digitizing oscilloscope (Tektronix TDS7254) must be applied. Even after these corrections the signal quality of the bunch profiles still remains at the limit of what is acceptable for tomography.

The phase space reconstructions of all bunches along the batch show that the bunch rotation applied prior to extraction from the PS is similar for all bunches along the batch as no significant variation of the tilt angle of the bunches is observed. Likewise, the longitudinal emittance of $\varepsilon_{\mathrm{RMS}} \simeq 0.1$ eVs along the

batch remains constant within the limits of the measurement precision. There is no significant difference between the emittance values measured with the two wall current monitors.

Several difficulties have been encountered during the analysis of the measurements in the SPS:

1. Even after the transfer function correction, the quality of the bunch profile measurements is at the lower limit of what is acceptable for tomographic reconstruction. Especially the tail and the ringing of the signal after the bunch should be suppressed further. The transfer function correction cannot be perfect (as the cable has high loss at high frequencies > 2 GHz) and it has been suggested either to digitize the beam signal in the tunnel close to the pick-up, or to transmit it to the surface using an optical fibre. Avoiding the long coaxial cables from the SPS tunnel to the surface is a crucial issue for the quality of the bunch profiles suitable for tomographic reconstruction.

2. The total RF voltage of the 200 MHz system in the SPS can be measured with a precision of about 10 %. Such an uncertainty can lead to a slightly wrong tilt angle of the reconstructed longitudinal distribution. As has been shown, this problem can be avoided by optimizing the tomographic reconstruction for best convergence, but only at the expense of added computation time.

3. The laborious post-processing of the mountain range data in the SPS needs to be replaced by an online application integrated into the control system, like those already operational in the machines of the PS Complex. In a first step, this application could be developed on the basis of PS Tomoscope, considering only the reconstruction of a single bunch. It could be extended later to the analysis of bunch trains. Furthermore, a dedicated oscilloscope or digitizer is required which is remotely controllable. The oscilloscope used to record the measurements described in this Note should remain available for MDs. A bunch synchronous burst trigger can be generated with standard modules of the SPS timing system.

Though only tentative measurements have been performed so far to show the feasibility and the performance of tomographic reconstructions of bunches in the SPS, they have resulted in interesting information on the longitudinal emittance and the tilt angle of bunches of an LHC beam right at injection. Further measurements under better conditions will certainly reveal more details of the longitudinal bunch distributions in the SPS.

A WC-2 wall current monitor and measurement system

The WC-2 wall current monitor installation consists of the pick-up AEW31731 as described in [5], a wide-band H-9 hybrid to combine the signals from the eight outputs of the pick-up and a transmission system, mainly a cable, to send the pick-up signal from the accelerator tunnel to the surface. The pick-up transfer function including the H-9 hybrid in frequency domain is derived from the step response of the pick-up in time domain which can either be measured or deduced from its geometrical configuration. In frequency domain, it becomes [6]

$$G_{\text{WC2}}^{\text{pick-up}}(\omega) = \left(1 - \frac{e^{-i\omega\tau_1}}{1 + i\omega\tau_2} \right) \frac{i\omega\tau_3}{1 + i\omega\tau_3}, \tag{2}$$

with $\tau_1 = 4.5$ ns, $\tau_2 = 40$ ns and $\tau_3 = 170$ ns. The transfer function of the transmission system has been derived on the basis of the measured attenuation versus frequency. It consists of several pieces of

coaxial cables, splitters, an attenuator and a switch. Neglecting an irrelevant delay factor, the cable is modeled according to the equations given in [4]

$$\frac{V_{\text{out}}}{V_{\text{in}}}(\omega) = e^{-\frac{al}{\sqrt{2\pi}}(1+i)\sqrt{\omega}} \cdot e^{-\frac{bl}{2\pi}\omega}, \tag{3}$$

where a and b are constants indicating the conductor and dielectric loss of the cable, l is its length and v is the group velocity of a signal in the cable. An additional, constant attenuation factor is multiplied to Eq. (3) to account for further elements like splitters and attenuators in the transmission system. Fitting the constants to the measured attenuation, results in the transmission system transfer function according to

$$G_{\text{WC2}}^{\text{trans}}(\omega) = 10^{a_1 - a_2(1+i)\sqrt{\omega} - a_3\omega}, \tag{4}$$

with $a_1 = -0.7937$, $a_2 = 2.294 \cdot 10^{-6} \sqrt{s}$ and $a_3 = 3.814 \cdot 10^{-11}$ s.

B   APWL-10 wall current monitor and measurement system

The measured transfer function of the new, LHC type APWL-10 wall current pick-up (APWL31732) is shown in Figs. 12 and 13 [7].   The frequency and phase response is nearly flat in the interesting
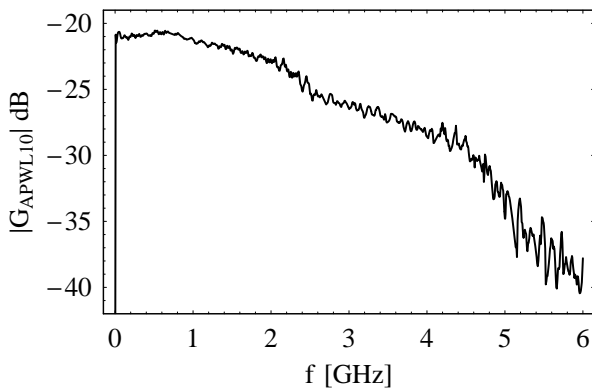

Fig. 12: Measured amplitude of the transfer function of the APWL-10 pick-up transfer function.
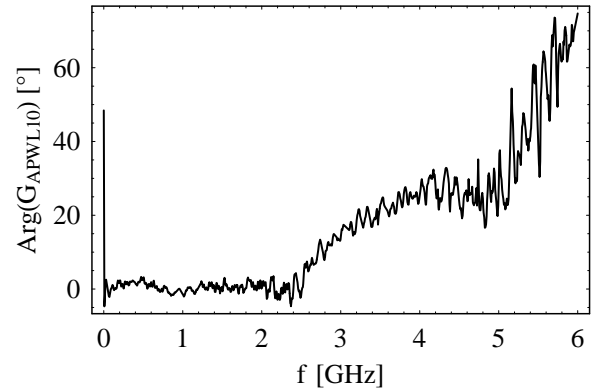
Fig. 13: Measured phase of the transfer function of the APWL-10 pick-up transfer function.

frequency range up to 2 GHz and no correction for the transfer function of this pick-up is required. The distortion of the signals from this pick-up comes mainly from the 200 m long 7/8" air dielectric ANDREW HJ5-50 cable. It can be modeled in the same way as the transmission system transfer function of WC-2:

$$G_{\text{APWL10}}^{\text{cable}}(\omega) = 10^{b_1 - b_2(1+i)\sqrt{\omega} - b_3\omega}, \tag{5}$$

with $b_1 = 2.755 \cdot 10^{-3}$, $b_2 = 4.603 \cdot 10^{-6} \sqrt{s}$ and $b_3 = 8.735 \cdot 10^{-12}$ s.

References

[1] S. Hancock, *A Simple Algorithm for Longitudinal Phase Space Tomography*. CERN PS/RF/Note 97-06, CERN, Geneva, Switzerland, 1997

[2] S. Hancock, P. Knaus, M. Lindroos, *Tomographic measurements of longitudinal phase space density*. European Particle Accelerator Conference, Stockholm, Sweden, 1998, pp. 1520-1522

[3] J.-F. Comblin, S. Hancock, J.-L. Sanchez Alavarez, *A Pedestrian Guide to Online Tomography in the CERN PS Complex*. CERN PS/RF/Note 2001-010 (revised), CERN, Geneva, Switzerland, 2001

[4] G. Brianti, *Distortion of Fast Pulses in Coaxial Cables*. CERN 65-10, CERN, Geneva, Switzerland, 1965

[5] T. Linnecar, *The High Frequency Longitudinal and Transverse Pick-ups used in the SPS*. CERN-SPS/ARF/78-17, CERN, Geneva, Switzerland, 1978

[6] T. Bohl, *Single short bunches at 26 GeV/c in SPS*. Note-2006-31, CERN, Geneva, Switzerland, 2006 (unpublished)

[7] T. Bohl, *APWL-10 transfer function*. Note-2006-37, CERN, Geneva, Switzerland, 2006 (unpublished)